GALACTIC AND EXTRAGALACTIC RADIO ASTRONOMY

CHAPTER 5

Supernova Remnants

D. E. Hogg

SUPERNOVA REMNANTS

Contents

5.1 INTRODUCTION

About ten years ago there was much work on the problem of supernova remnants in the Galaxy, and many remnants were identified, measurements of the integrated radio flux density were made, and theories of both the supernova event and the expansion of the remnant were postulated. Following this period, interest in supernova remnants waned, and the progress in the field was slow. Now, in response to a number of exciting new measurements, the field has again become the focus of much effort by astronomers. Among the new measurements the most important are the association of pulsars with supernovae; the detection of X-ray emission from a number of remnants; and the availability of high-resolution radio observations of both the total intensity and the polarized intensity from a large number of remnants.

The next section will describe the optical properties of supernovae, determined primarily from observations of extragalactic objects. Subsequent sections will describe the two best-studied remnants – the Crab Nebula and Cas A; the radio properties of remnants in the Galaxy; and the relationship between supernova remnants and cosmic rays.

Besides the more detailed references which will be cited throughout this chapter, there are a number of excellent surveys of the field, the most important of which are Minkowski (1968), Shklovsky (1968), the Crab Nebula Symposium at Flagstaff (summarized in Publ. Astron. Soc. Pacific 82, 1970), the IAU Symposium No. 46 on the Crab Nebula (1971), Milne (1970), Downes (1971), Ilovaisky and Lequeux (1972a,b), and Woltjer (1972).

5.2   OPTICAL PROPERTIES OF SUPERNOVA

5.2.1   Identification of Supernova Remnants in the Galaxy

As the early surveys of radio emission were compiled, it became clear that the radiation from the Galaxy was dominated by intense emission from a narrow region about the galactic plane, upon which were superimposed numerous discrete radio sources having angular diameters of one degree or less. Some of these had thermal spectra and were identified with prominent HII regions (Chapter 3) while others with nonthermal spectra were ultimately identified as remnants of galactic supernovae.

The association between supernova remnants and radio sources was initially suggested from the identification by Bolton, Stanley, and Slee (1949) of the radio source Tau A with the Crab Nebula, the remnant of a supernova observed by the Chinese and Japanese in AD 1054. Subsequent work strengthened the association by showing that the strong source Cas A was situated in a filamentary nebula having properties like those of supernova remnants, and by the successful search for radio emission in the regions of the supernovae of Tycho (AD 1572) and of Kepler (AD 1604). It is now reasonable to assume that all nonthermal galactic radio sources having diameters of a minute of arc or greater are remnants of supernovae.

The successful identifications of radio sources with SN1054, SN1572, and SN1604 encouraged an examination of the ancient astronomical records of the Chinese, Koreans, and Japanese, in hopes of finding other supernovae. Such records are very difficult to use because they are contaminated by observations of comets and novae which frequently cannot be distinguished because the necessary data on changes of position with time, or of magnitude

and duration of variability, are simply not available. Minkowski (1971) concludes that two other objects have been observed optically within the last 3000 years - the supernovae of AD 185 and of AD 1006. A number of other objects from the ancient catalogues have been suggested as super-novae, and a few of these might indeed gain general acceptance, but it is unlikely that the total number will exceed ten.

5.2.2 Types of Supernovae

Because there have been few outbursts observed in the Galaxy, the information about types of supernovae must come from the study of extra-galactic objects. The survey of galaxies for the purpose of finding super-novae has for the past thirty years been led by Zwicky, although a few very interesting objects have been found by chance by other observers. Photometric and spectroscopic observations of some of the 250 supernovae discovered shows that there are two principal types of supernovae.

Type I: This type is identified by its light curve, in which the time near maximum is about 50 days, and the subsequent decay is exponential, with the brightness decreasing by 1/e in 50 to 70 days. The photographic magni-tude at maximum, determined from the work of Kowal (1968), is given by $M_{pg} = 18.6 + 5 \log \frac{H}{100}$, where H is the Hubble constant. Also characteristic of this type is its color (relatively red, B-V between 0.5 and 0.9) and its spectrum, which in the initial stages shows broad overlapping emission bands. The initial velocity of expansion of the ejected material is in the range 15,000 to 20,000 km s^{-1}. Theoretical studies (Gordon (Pecker-Wimel) 1972) suggest that about 0.5 $M_{\odot}$ is ejected, and that the envelope is deficient in hydrogen.

Since all of the identified supernovae that have occurred in E or
SO galaxies belong to Type I, it is natural to assume that such supernovae
originate in stars of population II, of mass about 1.5 $M_\odot$. However, Type I
supernova also occur in the discs of Sb and Sc galaxies, in regions thought
to be predominantly of population I. One solution to this problem, proposed
by Tammann (1970), is that these supernovae result from collapsing white
dwarfs of an intermediate population.

Type II: The light curve shows great variations and cannot be used
alone for identification of the type. If photometry is available, these
objects can be distinguished by their ultraviolet excess. The best distinction
is by means of the spectrum, which at maximum is featureless, with a strong
blue continuum. The photographic magnitude at maximum, as determined by Kowal
(1968), is $M_{pg} = -16.5 + 5 \log \frac{H}{100}$. The ejected material shows velocities
of about 6000 km s^{-1}. By comparison with novae spectra, Shklovsky (1968)
estimates that as much as 1 $M_\odot$ is ejected in the shell.

Type II supernovae apparently result from extreme population I objects
having masses greater than 10 $M_\odot$, since they appear only in spiral or
irregular galaxies, often actually within spiral arms.

Zwicky suggests that, in addition, there may be three other less
common types, Types III, IV and V. These objects may simply be extreme
variations of the other types, but are so rare that their properties cannot
clearly be established. Thus Type III supernovae may be similar in nature
to Type II, except that a larger mass is ejected with a higher (12,000 km s^{-1})
velocity. Type V supernovae could be either dwarf supernovae or massive novae,
with velocities of only 2000 km s^{-1}.

5.3   THE CRAB NEBULA

5.3.1 Historical Summary

Throughout the study of supernova remnants the Crab Nebula has occupied a central position. The relationship between an observed supernova and visible nebulosity was established by the work of Duyvendak, Mayall,and Oort (1942), which conclusively identified the peculiar nebula M1, the Crab Nebula, with the supernova of AD 1054. Subsequently the nebula was identified as a radio source. Shklovsky (1954) proposed that the anomalous optical continuum from the Crab was synchrotron radiation, a proposal that was confirmed when the predicted optical polarization was discovered by Vashakidze (1954) and Dombrovsky (1954). Finally, the Crab Nebula was one of the first X-ray sources to be identified, and it is still the only supernova remnant showing an optical pulsar.

Because of its importance in the general study of supernova remnants, the Crab Nebula will be discussed in detail in this section. However, it must be emphasized that it has unique properties. The majority of the well-studied remnants are of a quite different nature, and are more nearly like Cas A, as will be shown in subsequent sections.

5.3.2 Optical Properties

The optical appearance of the Crab Nebula is dominated by an intricate network of sharp, well-defined filaments which have given it its name. Although the distribution of filaments in three dimensions is difficult to reconstruct, the filaments clearly are not confined to a thin shell at the periphery. The brightest filaments are distributed irregularly over the face of the object, and, in a few cases, extend radially outwards. The fainter filaments are found in almost all parts of a well-defined elliptical

region of dimension 3 minutes of arc by 2 minutes of arc.

Extensive studies of the radial velocities and proper motions of the filaments have been made by Trimble (1968). Measurements of both radial velocity and proper motion are available for 125 filaments, and these can be used to determine the distance of the nebula if the geometry of the filaments is known. Limits to the distance are obtained by assuming that the volume containing the filaments is either an oblate or a prolate spheroid. In the center the radial velocity is observed to be v_r = 1450 km s^{-1}. Along the major axis the largest proper motions are 0.22 arc secs yr^{-1}, and are fairly well-behaved, but along the minor axis there are large dispersions, with values up to 0.17 arc secs yr^{-1}. The distance in pc is then

$$D = \frac{v_r}{4.74\mu}, \quad v_r \text{ in km s}^{-1}, \quad \mu \text{ in secs yr}^{-1} \tag{5.1}$$

from which for an oblate spheroid having μ = 0.22, D = 1.4 kpc while for a prolate spheroid having μ = 0.15, D = 2.0 kpc.

Alternatively, instead of assuming a model for the geometry, Woltjer (1970a) has found the maxima in the distribution of both the proper motions and radial velocities, and concludes that the best value for the distance is 1.5 kpc. This is probably a lower limit, since the measurements of radial velocities are biased towards low values. In the following, a distance of 2.0 kpc will be used.

The proper motion studies of the filaments provide two other important facts about the nebula. First, if the motions are assumed constant and extrapolated back in time, the filaments converge in AD 1140, with an uncertainty of 15 years. Since this is significantly later than the outburst of AD 1054, the expansion must be accelerating. Second, the convergent point

of the nebulosity differs from the position of the pulsar, which in turn is generally accepted as being the stellar remnant of the supernova. The proper motion of the star is difficult to measure, apparently because many of the observations have been made with low angular resolution and are thus affected by the variable features in the nebulosity. However, the best estimate of the stellar proper motion is consistent with it being at the convergent point of the nebulosity in AD 1054.

The spectrum of the filaments is moderately rich in emission lines, with a number of hydrogen recombination lines as well as the lines of [OII], [OIII], [NII], [NeIII], HeI and HeII. With these lines it is possible in principle to determine the physical conditions in the nebulosity. The density is simply obtained from the ratio of the lines in the [OII] doublet at $\lambda 3729/3726$, and is about 1000 cm^{-3}. The temperature, total mass, and element abundance are much more difficult problems, since they depend both upon the differential absorption across the spectrum and upon the excitation mechanism. Davidson and Tucker (1970) have shown that a plausible model is obtained if it is assumed that collisional ionization is unimportant, and that the ionizing radiation originates in an ultraviolet continuum which smoothly joins the optical and X-ray data. In this case, the density of helium (including all levels of ionization) must be approximately equal to that of hydrogen, to explain the strong helium recombination line. That helium is seven times more abundant than in the interstellar medium in general suggests that the filaments were formed from enriched material ejected at the time of the supernova outburst. The temperature of the nebula drops from 15,000 °K at the center to 10,000 °K at the edge, and the total mass of ionized gas is $1.5 \, M_\odot$. It is also likely that some of the filaments have

cores in which the hydrogen is neutral; the mass of the neutral gas is not known.

Within the region outlined by the filaments is a bright continuum source, erroneously referred to as the amorphous component. Although generally elliptical in shape, the most intense emission comes from an "S"-shaped ridge along the major axis, and there are bays both to the east and west side where the emission is weak. It is also weak in the center, near the pulsar. Under best seeing, the emission appears to come from a complex pattern of very fine filaments which are of a different nature than the line-emitting filaments previously described.

The continuum emission was originally thought to originate in free-free and bound-free transitions in a highly ionized gas. However, the great difficulties with this mechanism - the large mass of ionized material re-quired, the absence of emission lines, the strong radio emission - led Shklov-sky (1954) to propose that the mechanism was synchrotron radiation. With the detection of polarization in the optical emission the synchrotron mechanism gained general acceptance, not only for the Crab Nebula but the other remnants as well.

The best summary of the optical polarization is still that of Woltjer (1958). In the central regions the polarization is 40 percent, rising to 60 percent in the outer regions. The direction of the polarized vector is more or less uniform over the central part of the nebula, and implies a magnetic field perpendicular to the bright ridge previously mentioned. In the outer parts the directions are more scattered, but there are a number of well-defined fans. The electric vectors in the fans are radial, suggest-ing a magnetic field around a current flow that is perpendicular to the plane of the sky.

The "amorphous" component has one other important characteristic. It has been known for fifty years that the details seen optically in the center of the nebula change with time. Recently Scargle (1969) has given a much more detailed description of these changes (Figure 5.1). The south-preceding star S1 is now identified as the pulsar. To the northeast of the pulsar are four well-defined filaments. The thin wisp nearest the star S1 moves in a quasiperiodic fashion, away and towards the star, with an apparent velocity of about 6×10^4 km s^{-1} and a time scale of 2 years. The motion of the other filaments is less regular, but it could represent either actual mass motion, in which the gas and field move together, or compressional waves which are generated near the star and move outwards.

5.3.3 The Spectrum of the Continuous Emission

In the frequency range 25-100 MHz most of the radio emission comes from an elliptical region centered on the optical nebula but larger, of size 5.5 x 3.5 minutes of arc. Within this region, in fact at a position (as determined by long-baseline interferometry) coinciding with that of the south-preceding star, is a strong point source with a peculiar spectrum. The source accounts for 20 percent of the total flux density at 38 MHz and 10 percent at 81.5 MHz. Between these two frequencies the spectral index is -1.2; at higher frequencies it must steepen to -2. Its size is uncertain, but scintillation measurements give a value of 0.2 ± 0.1 seconds of arc, implying that if the source is optically thick at 38 MHz, and is radiating by the synchrotron mechanism, then the magnetic field (from equation 12.22) is

$$B \sim 2 \times 10^{-5} \ \theta^4 \ \nu^5 \ S_m^{-2} \sim 10^{-6} \tag{5.2}$$

and the energy in particles alone would be 10^{50} ergs. Both of these values

seem unacceptable. An alternative explanation, that the source radiates

by plasma oscillations, is unattractive since the predicted high degree of

circular polarization has not been found. A more plausible suggestion, by Lang

(1971) and Drake (1970) is that the pulsar radio emission has been scattered

by the interstellar medium. The predicted values of source size and spectrum,

as well as the absence of pulses, are in general agreement with the observations.

Between 0.1 and 10 GHz high resolution observations are now becoming

available. Figure 5.2 shows a map of the total intensity at 2695 MHz, made

with the NRAO synthesis interferometer (Hogg, Macdonald, Conway, and Wade 1969) having

angular resolution of 10 seconds of arc. The nebula is still elliptical, but

smaller than at the lower frequencies. There is good agreement between the

optical and radio features; for example, the prominent optical bays have

radio counterparts, as does the ridge along the major axis of the ellipse.

Correspondingly detailed maps of the polarization at 2695 MHz also show

features similar to those at optical wavelengths. The degree of polarization

is about 10 percent near the center, and the polarization vectors have a

uniform direction in the region of the central ridge. There are in the

outer parts a number of distinctive features which clearly correspond to

the optical fans, but the orientations of the electric vectors are much

different, presumably because of rotation measures in excess of 300 rad m^{-2}.

For many years it was thought that the flux density increased by an

order of magnitude at millimeter wavelengths and fell again in the infrared.

Often, however, these early observations were not corrected properly for the

size of the source. Where only the best data are included, the spectrum

continues smoothly from decimeter wavelengths to optical wavelengths with
a spectral index of -0.26.

The characteristics of the optical emission have already been reviewed.
The apparent spectral index of the optical emission is strongly influenced
by the amount of extinction, which is not known accurately. If, for example,
the visual absorption is one magnitude, then the intrinsic optical spectrum
would fit smoothly to the infrared data, but the index would have steepened
to -0.9.

The Crab Nebula is a strong X-ray source which has been observed through-
out the range 1 keV to 100 keV. The spectrum of the radiation is hard,
although the spectral index of -2 is much steeper than at longer wavelengths.
A small fraction of the emission, ranging from 2 percent at 1 keV to 15
percent at 100 keV, is pulsed, indicating an origin in the pulsar. The
remainder of the X-ray emission comes from an extended region of diameter 100 seconds
of arc, the centroid of which lies near, but perhaps not coincident with, the
south-preceding star. The X-ray emission is probably Compton-synchrotron
emission from the nebula itself; in order that it be radiation scattered
from the pulsar there must be an unacceptably large amount of dust as well
as a large X-ray flux from the pulsar. That the average X-ray polarization
in the range 5-20 keV shows polarization of 15 percent (Novick et al. 1972)
is additional support for the synchrotron model.

The Crab Nebula itself has not yet been detected at energies above
1 MeV, although pulsed gamma ray emission has been observed. The upper
limits are consistent with the emission spectrum predicted by a Compton-
synchrotron model, in which optical and radio photons generated by the

synchrotron process are Compton-scattered into the gamma ray region. The limits to the gamma ray flux rule out the possibility that the high-energy electrons in the nebula are secondaries produced by the decay of π-mesons.

A summary of the spectrum of the Crab Nebula is given in Figure 5.3, taken from the work of Baldwin (1971). The synchrotron mechanism is the only radiation mechanism which provides reasonable agreement with the observations over this frequency range. The total power radiated is 1×10^{38} ergs s^{-1}, for an assumed distance of 2 kpc. The ultraviolet and X-ray region ($\lambda < 3000$ A) accounts for 63 percent of the radiated power, while 14 percent appears in the optical region (3000 - 10,000 A), 23 percent appears in the infrared (1μ - 1 mm), and only about 0.5 percent is emitted at radio wavelengths ($\lambda > 1$ mm).

5.3.4 The Crab Pulsar

The discovery of a pulsar in the Crab Nebula is one of the most important events in the study of supernova remnants, since the pulsar holds the key to the understanding of such diverse problems as the origin of the magnetic field in the nebula and the source of the relativistic particles which produce the observed emission. It was first observed as a radio pulsar by Staelin and Reifenstein (1968). They found, in the course of a survey for pulsars, an intense but highly variable pulsar (occasional peaks of 20,000 flux units have been observed at 430 MHz) with a pulse period of 33 msec. The period is not constant, but shows an increase of 36 ns per day. There have as well been at least two instances where the steady increase in period has been interrupted by an abrupt decrease, of about 100 ns.

Shortly after the discovery of the radio pulsar, Cocke, Disney and Taylor (1969) determined that the south-preceding star was optically pulsing in synchronism with the radio pulses. Figure 5.4 is the dramatic photograph by Miller and Wampler (1969), showing the absence of optical emission from the star between pulses. This star had long been known for its peculiar spectrum, which is continuous without recognizable absorption lines, and had been suggested by Scargle (1969) as the origin of the motions of the wisps.

Subsequent work has led to the detection of the pulsar in the infrared, X-ray and gamma ray wavelengths, and has given much detail about the shapes of the pulses, the dispersion measure and the amplitude variations. A more complete discussion is given in Chapter 6.

It should be noted that a second pulsar, NP0525, was found near the Crab, but it appears that it is not associated with SN1054, since the observed decrease in period is inconsistent with the large transverse velocity required.

The decrease in the period of the Crab pulsar inspired Gold (1969) to suggest that the loss in energy from the pulsar could supply the required energy for the nebula itself. From equation (6.3), it can be shown that the rate of loss of energy is

$$\frac{dE}{dt} = -I \cdot \frac{4\pi^2}{P^3} \frac{dP}{dt} \tag{5.3}$$

with I the moment of inertia and P the period.

For a star of one solar mass and diameter 10 km, values thought to be typical of a neutron star, equation (5.3) predicts a loss of 4×10^{38} ergs s^{-1}, to be compared with the radiative loss of 1×10^{38} ergs s^{-1} from the nebula.

At this time there is no agreement as to how the energy released by the star may be coupled to the nebula. It is generally accepted that the pulsar is a rotating magnetic neutron star with a corotating magnetosphere. The star may be surrounded by a relatively dense plasma. Particles escaping from the magnetosphere could be accelerated to high energy by magnetic dipole radiation, as has been suggested by Ostriker and Gunn (1969), or they may be accelerated electrostatically by a component of the electric field parallel to the magnetic lines (Goldreich and Julian 1969). Another interesting suggestion concerning the period decrease, or "spinup", has been made by Pacini (1971). Shortly after the event in 1969, there was some evidence that the structure of the wisps changed. The change in rotational energy of the star is insignificant, but perhaps there was a major temporary change in the structure of the magnetosphere, permitting the release of up to 10^{43} ergs of plasma energy. Pacini suggests that such an event might occur every year or two, in agreement with the time scale observed for the motion of the thin wisp.

Clearly much more work is required on the various theories, but already the close relationship between the pulsar and the physical conditions in the nebula has been established.

5.4 THE REMNANT CASSIOPEIA A

5.4.1 Optical Properties

The optical object associated with the strong radio source Cas A (3C 461) was first identified by Baade and Minkowski in 1954. The best existing plate shows that the optical nebulosity forms an incomplete shell of diameter 4 minutes of arc, with a large number of small knots located to the north and northeast of the

apparent center of expansion. Fainter and more diffuse filaments are located in the southern part of the shell. In the east the shell is broken, and a flare extends outwards to a distance of about 4 minutes of arc.

The filaments and knots are of two distinct types: about 30 are very red and show radial velocities of only 30 km s^{-1}, while the other hundred are much bluer, and have either large radial velocities of up to 6000 km s^{-1} or large proper motions. In a recent study of the high-velocity knots, van den Bergh and Dodd (1970) have shown that the motions are consistent with the theory that the knots originated at the same time, in AD 1667, and have not suffered significant deceleration. There is no stellar remnant brighter than m $\sim$ 23.5 at the position of the center of expansion. The distance is uncertain by about 10 percent; the observed proper motions of 0".5 yr^{-1} combined with an expansion velocity of 7400 km s^{-1} lead to a distance of 3 kpc, which is consistent with the hydrogen 21 cm absorption profiles that have been observed.

The origin of the flare at the east is unknown. If it is as old as the filaments and knots in the rest of the shell, then the shell itself must be severely retarded, which is inconsistent with the analysis of proper motions. Moreover, the initial velocity must have been in excess of 30,000 km s^{-1}, larger than that observed for any other supernova. Alternatively, Minkowski (1968) suggests that two shells have been ejected, at much different velocities, and that the flare is the only surviving part of the high velocity shell, while the system of knots shows the location of the slower shell. Such an expansion has been observed in the Type III supernova in NGC 4303.

It is an interesting question as to why this supernova was not observed visually by the European astronomers, since to them the object is circumpolar. A typical supernova of Type II has a visual magnitude at maximum of -18, for a Hubble constant of 50 km s^{-1} Mpc^{-1}. In the absence of absorption the supernova would have attained an apparent magnitude of -6, too bright to have been overlooked. However, if the visual absorption is as much as 7 magnitudes, as measurements by van den Bergh suggest, then the maximum visual magnitude would have been less than +1, sufficiently faint that it could have been missed.

The lifetimes of the moving knots are short, on the order of ten years, with the smallest structures changing even within one year. New knots are continually being formed in the regions in which knots are already present, so that the general shell-like appearance of the source is maintained.

Spectra of the stationary filaments show lines of Hα and [NII], with very weak lines of [OII]. According to Peimbert and van den Bergh (1971) this requires that nitrogen must be overabundant relative to oxygen if the filaments are ionized by radiation. Thus, these filaments might be formed by compression of enriched circumstellar material which was present before the supernova event.

The fast-moving knots have a much richer spectrum, characterized by the forbidden lines of O, S, and Ar. Lines of H and N are absent. Assuming that the total visual absorption is 6 magnitudes, Peimbert and van den Bergh conclude that the abundance of oxygen is anomalously high, by a factor of up to 70, relative to nitrogen and hydrogen. This is the best direct observational evidence for the hypothesis that heavy elements are synthesized in supernova outbursts.

The line ratios also reflect the physical conditions within the knots. The electron temperature is 15,000 °K, the electron density is 1×10^4 cm^{-3}, and the mass of the moving knots visible at the present time is ~ 0.25 $M_\odot$. It is not known how much of the shell is neutral; if the shell were complete, the total mass could be as high as 2 $M_\odot$.

5.4.2 Radio Properties

As the brightest source in the radio sky, with the exception of the Sun, Cas A has been studied extensively at a large number of wavelengths. Between 22.5 MHz and 14 GHz the flux density decreases with frequency, with a spectral index of -0.77. Below 18 MHz the flux density decreases with decreasing frequency, with an index of +1.6. The most likely explanation of the turnover at low frequency is absorption by free-free transitions either in the interstellar medium or within the source. A consistent picture for Cas A and a number of other sources showing a similar turnover requires that the absorption be in the interstellar medium. The low frequency spectral index is too steep to be explained by a cutoff in the energy spectrum of the electrons which produce the synchrotron radiation; too much of the radiation comes from regions of angular size 40 seconds of arc or greater, ruling out the possibility that there is significant self-absorption (cf. Chapter 12); and the Tsytovich-Razin effect could be important in the filaments where the density is high, but requires too small a magnetic field to be important for the bulk of the source.

The distribution of total intensity of radiation from the source has been mapped at frequencies between 1400 MHz and 5000 MHz, with resolutions between 24 and 7 seconds of arc. The observed distribution is consistent with an emitting shell

of thickness 0.4 pc and outer radius 1.9 pc. Figure (5.5)

from Hogg et al. (1969) shows a map of the source at 11 cm, and the re-

lationship to the optical nebulosity. The shell contains many discrete

regions of angular scale 10" or less which lie towards the edge of the

source and show little connection with the optical filaments. At 5000 MHz

about 9 percent of the total radiation comes from these small features

(Rosenberg 1970).

In all of these maps, the region of the flare containing the high-

velocity filaments is characterized by a break in the radio shell. The work

of Rosenberg suggests that the spectral index, uniform over the bulk of the

source with value -0.75, may be flatter in this region, with value -0.6.

There is also a suggestion of an extension in the contours of low-intensity

emission. It is interesting to note that at meter wavelengths Jennison (1965)

has found a spur whose spectrum might be very steep, thereby favoring low

frequency emission. It will be important to settle the question of the

spectral index of the spur, and to measure it at low frequency with higher

sensitivity and angular resolution.

The total power radiated by Cas A in the frequency range up to 100 GHz,

is 4×10^{35} ergs/s, assuming a distance of 3 kpc. The total energy radiated

over the lifetime of this object, if the rate had been unchanged, is

4×10^{45} ergs. This is a small fraction of the total energy in relativistic

electrons - 10^{49} ergs - as calculated by Rosenberg. An estimate of the

magnetic field (assumed to be uniform throughout the shell) is obtained by

assuming that equipartition between particle energy and magnetic field energy

obtains; the field is thus 5×10^{-4} gauss. In the small, more intense regions

of radio emission, the emissivity is approximately 100 times greater than in

the shell, and the field is twice as strong.

Mayer and Hollinger (1968) discovered several years ago that the radio emission from Cas A was significantly polarized, but that it was so symmetric that there is substantial cancellation of the integrated polarization unless the observations are made with high resolution. Two such high-resolution maps -- by Rosenberg (1970) at 6 cm and by Downes and Thompson (1972) at 11.1 cm -- are now available. The polarized radiation is mainly concentrated in the bright ring of the source and amounts to about 5 percent of the unpolarized flux density. Although the data are as yet sparse, Downes and Thompson show that the complex patterns of depolarization and Faraday rotation could be explained by a magnetic field consisting of a uniform radial component of strength 1.6×10^{-4} gauss and a random component of rms strength 5×10^{-4} gauss. If the depolarization occurs in the shell, then the required electron density is 2 cm^{-3}, and the total mass of the shell is $1.2 \, M_\odot$. This mass is in addition to the mass contained in the optical filaments, since the filaments occur predominantly in the northwest, while the depolarization is important in the other quadrants.

5.4.3   Secular Changes in Intensity and Structure

A decade ago Shklovsky (1960) showed that the flux density of a homogeneous expanding nebula should decrease with time, and that for an especially young object, such as Cas A, the change should be readily observable.

If a source is radiating by the synchrotron mechanism, the flux density S_ν will be related to the radius r_o of the radiating volume and the

magnetic field strength $H_{o\perp}$ by

$$S_\nu \ \alpha \ r_o^3 \ K_o \ H_{o\perp}^{\frac{\gamma+1}{2}} \ \nu^{\frac{1-\gamma}{2}} \ , \tag{5.4}$$

where the energy spectrum of the radiating electrons is

$$dN(E) \ = \ K_o \ E^{-\gamma} \ dE \ .$$

As the source expands to a radius r, and assuming both that the magnetic flux remains constant and that the particle energy is limited by statistical acceleration, the following relations obtain:

$$H \ = \ H_o \left(\frac{r_o}{r}\right)^2$$

$$E \ = \ E_o \left(\frac{r_o}{r}\right)$$

$$\gamma \ = \ \gamma_o \tag{5.5}$$

$$K \ = \ K_o \left(\frac{r_o}{r}\right)^{\gamma-1} \left(\frac{r_o}{r}\right)^3 \ .$$

Thus the flux density at any later time is simply

$$S_\nu \ \alpha \ r^{-2\gamma} \ . \tag{5.6}$$

Actually Cas A is not a uniform sphere, but rather a shell source. For an expanding source in which the shell thickness remains constant, Kesteven (1968) finds that the equation is modified slightly, to become

$$S_\nu \ \alpha \ r^{-\frac{1}{2}(3\gamma-1)} \ . \tag{5.7}$$

The annual decrease in flux density is then

$$\frac{\Delta S_\nu}{S_\nu} = - \frac{\frac{3\gamma-1}{2}}{T} .$$

(5.8)

For Cas A, $\alpha = \frac{1-\gamma}{2} = -0.77$; $\gamma = 2.54$; and $T = 305$ years. The annual decrease predicted by equation (5.8) is 1.1 percent, in good agreement with the observed value of 1.3 ± 0.1 percent (Scott, Shakeshaft and Smith 1969).

If the radio shell is expanding at the rate given by the proper motions of the optical filaments, it should be possible to see changes in the source structure. Rosenburg has compared maps made at Cambridge over a time interval of 3 years, with inconclusive results. In the near future, as the time interval approaches ten years, it seems likely that significant structural changes will be observed.

5.4.4 X-Ray Emission from Cas A

This remnant has been detected as a source of X-rays in the energy range $1 \leq E \leq 10$ keV. As yet high angular resolutions are not possible, so that the structure of the X-ray source is not known. It has a hard spectrum, with a spectral index equivalent to -3.3. The flux density ranges from approximately 2×10^{-29} wm^{-2} Hz^{-1} at 1 keV to 2×10^{-31} wm^{-2} Hz^{-1} at 10 keV, or about a factor of 10 less than the X-ray flux from the Crab Nebula. The radio spectrum extrapolates to meet the X-ray flux at 1 keV.

It is not yet possible to determine the origin of the X-ray emission. That the radio flux extrapolates to meet the X-ray flux suggests that the X-ray emission could simply be high-energy synchrotron emission. Alternatively, the expanding shell source might have sufficiently high temperature to produce

thermal X-rays. The question of the origin of the radiation is quite critical,
because of the short lifetimes involved. For example, equation (12.7) shows
that the power radiated by a relativistic electron is

$$\frac{dE_{Gev}}{dt} = - A\, B_{\perp}^2\, E_{Gev}^2 \quad Gev/sec \tag{5.9}$$

from which the half-life is

$$t_{1/2} = \frac{1}{A\, B_{\perp}^2\, E_{Gev}} \quad sec \tag{5.10}$$

with $A = 3.80 \times 10^{-6}$. For a field of 10^{-4} gauss and X-radiation at 10^{18} Hz,
the particle energy from equation (12.6), assuming radiation at $0.28\, \nu_c$, is
4.6×10^4 Gev. Equation (5.10) then predicts for such a particle a life-
time of 20 years, requiring that injection of such particles must still be
occurring.

5.5 SUPERNOVA REMNANTS IN THE GALAXY

5.5.1 Some Well-Studied Remnants

There are now more than 90 objects which have been identified as super-
nova remnants or as possible remnants. Catalogues of these objects have
been compiled most recently by Milne (1970), by Downes (1971), and by
Ilovaisky and Lequeux (1972a). Attempts to detect hydrogen recombination line
emission from many of these objects have been made, and a number of HII
regions which were misidentified have been found (cf. Dickel and Milne 1972),
but the majority are nonthermal galactic sources. There are as yet no data
as complete as those available for the Crab Nebula and Cas A. Hopefully
in the near future better maps of radio polarization, more detections of
X-ray emission, and more spectroscopic studies of visible nebulosity will

be obtained for a large number of remnants. Even now, however, there are

sufficient data to reveal some general properties of supernova remnants.

The basis of the discussion of the properties of supernova remnants

is the group of sixteen objects for which a distance has been estimated.

The accuracy of the distance estimate varies greatly from source to source.

For example, the three objects for which optical proper motions are avail-

able -- the Crab Nebula, Cas A, and the Cygnus Loop -- are at distances

known to better than 20 percent, while only a lower limit, based on neutral

hydrogen absorption, is available for Tycho's supernova. Other techniques

used are the association of the radio source with a star cluster of known

distance, the estimation of the distance modulus from the observed optical

maximum, and the amount of interstellar absorption at low frequencies. The

properties of these objects, adapted from the work of Ilovaisky and Lequeux

(1972a), are given in Table 5.1.

A number of these objects are deserving of further comment:

SN 1572 (Tycho's supernova, 3C 10). This object was observed by Tycho

Brahe in 1572, when it attained a maximum apparent magnitude of -4. The

observations of the light curve and color suggest that it was a supernova

of Type I, and in fact Minkowski (1968) considers it to be a prototype of

this class.

The remnant is seen as two filaments and an arc which are symmetric

enough to allow determination of the center of expansion. The observed radial

velocities are very low, presumably because the filaments are near the edge.

Van den Bergh (1971) has found that the proper motions are 0.2 seconds of arc yr^{-1},

corresponding to a velocity of 4700 km/s at a distance of 5 kpc. Since the

observed proper motion is less than one-half that required if the nebula were expanding uniformly, the shell must be strongly decelerated. If the deceleration has been caused by interstellar matter of density 1×10^{-24} g cm^{-3}, then the mass of material already swept up is 12 M_o, and the initial velocity must have been $\sim$ 20,000 km s^{-1}.

The radio source has a shell structure, with a very sharply defined outer edge. The optical filaments lie close to the edge of the radio source. The thickness of the radio shell is about one-quarter of the outer radius. Observations of the polarization at 1420 and 2880 MHz by Weiler and Seielstad (1971), and at 2695 MHz by Hermann (1971) reveal that the field is primarily radial in direction, and is highly ordered, with the polarization generally about 10 percent, but rising to 20 percent in some regions. Figure 5.6, from the work of Weiler and Seielstad (1971), shows the distribution of the intrinsic position angle of the electric vector for this source.

Recently this remnant has been detected as an X-ray source. It has a relatively hard spectrum, comparable with that of Cas A.

SN 1604 (Kepler's supernova, 3C 358). In 1604, Kepler noted the appearance of this object, with a maximum apparent magnitude of -2. Although the data are not as good as for SN 1572, the supernova was probably of Type I. There are several filaments showing Hα, [NII], and [OI] with normal intensity ratios. The observed radial velocities are in the range 200-300 km s^{-1}. These low velocities are very puzzling, in view of the short time available for deceleration. They imply either that the density of interstellar matter is very much greater near SN 1604 than it is near Cas A, for example, or that the filaments are analogous to the low-velocity features in Cas A, and may therefore be compressed circumstellar material, as has been suggested by van den Bergh.

Little is known about the radio structure of this source. The recent work by Hermann at 2695 MHz shows that it is probably a shell source, with the fractional polarization reaching a maximum of 10 percent near the center. The limited polarization data are consistent with a radial magnetic field.

The Cygnus Loop. This is a famous object showing well-developed filamentary structure. The northeast region is so bright that it is identified separately in the NGC catalogue as NGC 6992/95.

Studies of the spectrum by Parker (1964) have led to the conclusion that the filaments are actually thin sheets of nebulosity seen edge-on. There is evidence for temperature stratification behind a shock front. The presence of [OIII] lines is best explained by a region with temperature greater than 50,000 °K while lines arising from H, N, and S require temperatures of only 20,000 °K. The abundance of these atoms is normal if stratification is assumed. The total mass of the visible nebulosity is $2 \ M_\odot$, a small fraction of the 100 $M_\odot$ which might have occupied the volume that has now been swept out. Parker concludes that the distribution of visible filaments is closely related to the distribution of interstellar material with which the expanding shell can interact. The density of the interstellar clouds will govern the level of ionization and the temperature behind the shock front.

From the proper motions and radial velocity of the filaments the distance is 770 pc and the age, allowing for deceleration, is 70,000 years.

The radio emission from the Cygnus Loop (Figure 5.7) shows good correspondence with the optical nebula, especially in the region of NGC 6992/95; there may be significant thermal radiation from the filaments there. There is a prominent source outside the shell at the southwest. In this region

the shell is broken, and the source there might represent the loss of energetic particles from the nebula. This source, and the neighboring region in the shell, are the only places where Kundu (1969) found significant polarization at 11 cm. The polarization ranges between 15 and 25 percent, and, if the Faraday rotation is small, shows that the magnetic field is aligned along the filaments.

The Cygnus Loop has been identified as an X-ray source having a spectrum that is much softer than that of Cas A or SN 1572. The X-ray structure measured by Gorenstein et al. (1971) has the same angular size as the outermost boundaries of the optical filaments, and is more or less constant across the circular region defined by the filaments. This is in contrast to the radio emission.

5.5.2 The Radio Properties of Supernova Remnants.

In recent years, due in large part to the work of Milne, Dickel, Kundu, and Downes, the structure in both total intensity and in polarization has been measured for a large number of remnants. In total intensity, eighty percent of the objects which have been studied with high resolution show definite shell structure, or at least enhanced brightness at the edge of the source. The remainder could be similar to the Crab Nebula, although with very much lower surface brightness. Amongst the shell sources the thickness of the shell ranges from 10 percent to 30 percent of the diameter; Milne (1970) concludes that as the remnants expand, the ratio of the shell thickness to diameter remains constant.

A large number of remnants have polarized emission in which the direction of the electric vector is quite confused, so that there appears

to be no systematic magnetic field. Many objects, amongst them the youngest remnants (Cas A, SN 1604, SN 1572, and SN 1006) have a highly ordered radial magnetic field. Seven others, generally with diameters greater than 15 pc, clearly have the magnetic field directed around the periphery of the shell. The picture that emerges is that the field in the younger remnants is radial, presumably a result of the general outflow of material in the expansion. As the expansion proceeds, regions in which the field is tangential are formed by the interaction of the shell with the interstellar medium. Since this latter process is dependent not only on the energy and mass distribution of the shell but also on the strength and orientation of the interstellar field, it is to be expected that remnants in this stage will show a confused field pattern, with both tangential and radial components present.

The spectral indices of the emission from remnants ranges between -0.1 and -0.8, with a mean value of -0.45. Most remnants have straight spectra over the observable range, except for the absorption at low frequencies by interstellar matter. Suitable observations are not generally available to determine if there are spectral index changes within a source, but it is clear, for example, that in the Cygnus Loop the spectrum of the emission from NGC 6992/95 is curved, and is different from that of other parts of the source. Contrary to early suggestions, there is no change in radio spectral index as the remnant expands.

5.5.3 Evolution of Supernova Remnants

It is to be expected from equation (5.6) or (5.7) that the flux and surface brightness of a supernova remnant will decrease as it expands into the interstellar medium. Since for most objects the decrease in flux will

be undetectable, even over a decade, a number of authors have instead

attempted to measure the change of flux with size. Some have plotted the

distance-independent quantity surface brightness as a function of angular

diameter; there will, however, be some scatter introduced by the implicit

assumption that all remnants are at approximately the same distance,

whereas in fact they range over distances differing by a factor of 10.

The most useful plot is that of surface brightness against linear diameter

for the source of known distance (Table 5.1) because if a relationship

can be established, then it can be used to find the distances of those

objects for which surface brightnesses and angular diameters are known.

Figure 5.8 shows the surface brightness-linear diameter relationship

for the objects of Table 5.1. Although there is considerable scatter,

there is a definite decrease of surface brightness Σ with increasing

diameter D. If the sources Kepler, MHR44, 3C397, W44, IC443, SN1006, and

HB3 which have large uncertainties in D are given one-half weight, and

omitting the Crab Nebula, then the least-squares solution yields

$$\Sigma \propto D^{-3.7 \pm 0.4}$$
(5.11)

A part of the scatter in Figure 5.6 is due to the uncertainties in the

observations. Most serious are the uncertainties in the distances, where

the most accurate (Cas A, Tau A, Cygnus Loop) are no better than 10 percent,

while in the worst cases the possible error approaches 50 percent. The

errors in surface brightness are less than 10 percent for the sources of

high surface brightness, where the angular diameter can be accurately defined,

but rise to perhaps 30 percent for a source like HB3.

The scatter in Figure 5.8 is greater than that expected from these errors,

however, showing that there is an intrinsic dispersion amongst the sources

themselves. Certainly the extragalactic supernovae show a range of velocity of the ejecta, and it is to be expected therefore that the galactic super- novae will have a similar dispersion in velocity, and perhaps in initial energy as well. In addition, the latter stages of evolution, even for objects which were initially identical, might be different because of differences in density of the ambient material into which they expand. Finally, it is known that in the Crab Nebula relativistic particles are still being injected 900 years after the supernova event. If continuing injection occurs in other cases as well, it must have a profound effect on the surface brightness-linear diameter relationship, leading for example to a parallel sequence of objects like the Crab Nebula.

From the Shklovsky relation [equation (5.6)] the surface brightness will be related to the linear diameter by

$$\Sigma \propto D^{-2\gamma-2} = D^{4\alpha-4} \tag{5.12}$$

which for a typical spectral index of -0.5 gives $\Sigma \propto D^{-6}$, much steeper than is possible from equation (5.11). Similarly, an expanding shell can also be ruled out. A remnant expanding with a shell of constant thickness requires $\Sigma \propto D^{-4.5}$ from equation (5.7), which is included within the un- certainty of (5.11); such objects are probably excluded since the remnants of low surface brightness have relative shell thicknesses that are comparable to or larger than those of the remnants with high surface brightness. Thus the surface brightness - diameter relationship [equation (5.11)] leads to the conclusion that the majority of the remnants observed are in a phase where the interaction with the surrounding medium has become important (van der Laan 1962, Poveda and Woltjer 1968).

Several distinct phases in the evolution of a supernova remnant can now be identified, and are described by Woltjer (1972) and by Ilovaisky and Lequeux (1972a). Initially the remnant expands freely, as a result of the outburst, in the manner described by Shklovsky. This stage is quite short-lived -- Woltjer estimates perhaps 100 years -- because quite rapidly the expanding remnant sweeps up interstellar matter of total mass much greater than the mass initially ejected. During the second phase the expansion is adiabatic, and could lead to the development of shell sources of radio emission as envisioned by van der Laan. Most remnants observed are in this phase. For example, Tycho's supernova has entered this phase after only 400 years, while the X-ray emission from large remnants with low surface brightness such as the Cygnus Loop shows that the radiative cooling which terminates this phase has not yet become important. Thus the second stage may last as long as 7×10^4 years. The final stages of evolution are only defined theoretically, since there are no known remnants definitely identified with them. The shell might continue expansion at constant radial momentum, or it might be forced to expand by the pressure of cosmic rays trapped within the remnant. In either case the source will ultimately become indistinguishable from the galactic radio background.

A completely different mode of evolution in which the decrease of radio emission is ascribed to the decrease in particle injection by a central pulsar has been proposed by Pacini (1971). In this theory, all supernova remnants have pulsars which are a source of continuous injection of relativistic particles. In a remnant such as Cas A, the pulsar period is predicted to be long and the pulsar accordingly would be difficult to detect. The magnetic field near the postulated pulsar would be weak, and the ejected particles

would emit significant synchrotron radiation only in an outer shell where the interstellar field has been compressed during the expansion of the remnant. Thus the difference in structure between the shell sources and the more uniform ellipsoids like the Crab Nebula is attributed to the property of the central star.

This theory is difficult to assess, since repeated searches of supernova remnants have failed to find associated pulsars, except in the three instances discussed below. The surface brightness - diameter relationship in equation (5.11) is of little value, since the relationship predicted in Pacini's theory depends critically on certain properties of pulsars which are not yet known. However, even if there is continuing injection of particles, the remnants must pass through the three expansion stages described above, although the time spent at each stage might be increased over the case where there is no injection after the initial event.

A potentially more sensitive method of studying the final stages of evolution is by determination of the luminosity function. In the most complete discussion at this time, Ilovaisky and Lequeux (1972a) find that for remnants having diameters between 10 pc and 25 pc, within 7.6 kpc of the Sun, the number having diameter less than a given value is

$$n(<D) \propto D^{3.2 \pm 0.7} .$$

(5.13)

The luminosity function for remnants having diameters greater than 30 pc is dominated by observational selection effects, since such objects cannot easily be identified against the galactic background. On the other hand, there are too few objects with diameters less than 30 pc to permit an accurate determination of the number-diameter relationship; the observed

exponent, 3.2±0.7, cannot distinguish whether the remnants are in the

deceleration phase (exponent value is 2.5), the constant radial momentum

phase (exponent is 4), or the cosmic ray pressure phase (exponent is 3).

Since there is little hope of increasing the number of identified remnants

significantly, Ilovaisky and Lequeux conclude that the luminosity function

has little value in the study of the evolution of supernova remnants.

5.5.4 Distribution of Remnants in the Galaxy

The location of all of the presently identified remnants can be

determined by using equation (5.11) to estimate the distances. The remnants

are concentrated towards the Sun because of observational selection effects

that are especially serious for objects of low surface brightness. An

estimate of the completeness of the sample can be made by assuming that

the luminosity function equation (5.13) applies not only near the Sun but

throughout the Galaxy as well. In this way Ilovaisky and Lequeux (1972a)

find that the surface density of remnants with diameters less than 30 pc

is approximately constant as a function of distance from the galactic center

out to 8 kpc, with a value of 0.5 kpc^{-2}, after which the surface density

drops rapidly, with no remnants lying beyond 16 kpc. The total number

expected in the Galaxy is only 200, so that nearly half of the entire

population has now been identified.

The remnants are strongly concentrated towards the galactic plane,

although the scale height of the distribution increases with increasing

distance from the galactic center; the scale height near the sun is 90 pc.

Milne (1970) has found that within the plane the remnants are found

preferentially in the neutral hydrogen concentrations of the spiral arms.

It is clear therefore that the distribution of remnants within the Galaxy is similar to the distribution of extreme population I objects. They must result from supernovae of Type II (or possibly of Type III). It is tempting to postulate that since the majority of remnants are shell sources like Cas A and the Cygnus Loop, the shell structure is a characteristic of the Type II supernova. Sources like the Crab Nebula and 3C 58 could be remnants of a fundamentally different type of event. However, both Tycho's supernova and Kepler's supernova are believed to have been of Type I, and the remnants of these also have a shell structure. Apparently present data are not sufficient to uniquely classify the type of supernova that led to a given remnant. Some other criterion, such as the spectroscopic characteristics of the filaments in the remnant, must be developed.

There is considerable interest in the comparison of the galactic distribution of supernova remnants and of pulsars, in order to test the hypothesis that pulsars are the stellar remnants of supernovae. The best evidence of an association would be to find pulsars actually in supernova remnants, but after many searches there is still only one well-established association (the Crab pulsar) and two possible associations (pulsar 0833-45 with Vela X and pulsar 1154-62 with G 296.8 - 0.3 in Crux). This lack of detailed correlation might arise because the surveys for pulsars, especially of short period, are not complete; because the radiation from pulsars is sharply beamed; or because there is no real association. To evaluate this last possibility, Iloviasky and Lequeux (1972b) have studied the galactic distribution and density of pulsars. They confirm the earlier results that the scale height of the pulsar distribution near the sun is 120 pc, comparable with that of the supernova remnants. The surface density of pulsars of age

less than 5×10^6 yr is about 100 kpc^{-2}, or 200 times greater than the surface density of remnants having diameters less than 30 pc and ages less than 1×10^4 yr. Since the surface densities are approximately in the same ratio as the lifetimes of the two classes of objects, it is concluded that the density and distribution of pulsars is consistent with their origin being in the same type of event that produced the supernova remnants.

5.5.5 Input of Energy to the Galaxy

It has long been felt that supernovae could be a significant source of energy for the Galaxy, with the energy transmitted both in the form of cosmic rays and in kinetic energy of the expanding remnant. Now that the properties of remnants are better understood, it is useful to estimate the amount of energy potentially available from these objects.

The initial energy of the supernova outburst must be greater than $\sim 10^{49}$ ergs, the total amount of light emitted near maximum (Minkowski 1968). Another lower limit is obtained from the kinetic energy of the expanding shell. For a remnant like the Cygnus Loop, which has entered the deceleration phase, the diameter D is given as a function to time t, energy of the outburst E, and density of the surrounding medium ρ by (Woltjer 1970b)

$$D = 2.34 \frac{E}{\rho}^{1/5} t^{2/5} . \qquad (5.14)$$

For the Cygnus Loop, D = 42 pc and $t \sim 5 \times 10^4$ years. Assuming $\rho \sim 1 \times 10^{-24}$ g cm^{-3}, $E = 2 \times 10^{50}$ ergs. This value is critically dependent on the density of the interstellar matter, and could be as low as 5×10^{49} ergs. Other remnants also appear to require initial kinetic energies in the range $10^{49} - 10^{50}$ ergs.

These values are lower limits, because it is not known at what efficiency the initial energy of the outburst can be converted into either optical energy or kinetic energy. Presumably the supernova outburst occurs as a result of evolution of the core of a star to a density of $\sim 10^{11}$ g cm^{-3}, at which point a dynamic implosion occurs, in the manner described, for example, by Colgate and White (1966). The implosion ultimately leads to an outgoing shock wave which can eject the envelope of the star with a kinetic energy of at least 10^{50} ergs, the amount required by equation (5.14). The explanation of the optical flash is more controversial. On the one hand Morrison and Sartori (1969) propose that the optical emission is neither from the supernova itself nor from the envelope, but rather is from a large HII region excited by a pulse of ultraviolet radiation. Such a model would require that the total energy in the event be $\sim 10^{52}$ ergs for a Type I supernova, and 10^{50} ergs for a Type II supernova. Colgate (1972) on the other hand proposes that the excitation of the HII region results from the conversion of the kinetic energy of the ejected shell; this also requires $\sim 10^{52}$ ergs. Thus, although the nature of the outburst is not yet understood, the total energy involved is 10^{51} - 10^{52} ergs, of which 1 to 10 percent appears as kinetic energy in the remnant.

Equation (5.14) can also be used to estimate the frequency of occurrence of supernovae in the Galaxy. There are 170 remnants in the Galaxy having diameters less than 25 pc (Ilovaisky and Lequeux 1972a). These must have ages less than 1.4×10^4 years from equation (5.14), assuming that $E/\rho = 2 \times 10^{74}$, the value for the Cygnus Loop. Thus the mean interval between supernovae is 80 years. The value obtained here is slightly higher than the 60 years obtained in a number of other studies; the difference perhaps lies in the

value of E/ρ adopted.

With these numbers, it is now possible to estimate the amount of energy available from supernovae. The energy appearing as kinetic energy in the expanding remnant is 8×10^{40} ergs sec^{-1}, while the energy available from the initial ultraviolet flash amounts to $\sim 10^{42}$ ergs s^{-1}. This latter amount is large enough to be of critical importance to the thermal and ionization balance of the interstellar gas (Jura and Dalgarno 1972).

Supernovae and their remnants have also been postulated as the primary source of cosmic rays in the Galaxy. To maintain the present energy density of 1×10^{-12} erg cm^{-3} requires a continual injection of $\sim 6 \times 10^{40}$ erg s^{-1} (Woltjer 1970b) for all cosmic rays, and about one hundredth of that for the electron component. The observed remnants have an energy in relativisitic electrons of $\sim 5 \times 10^{48}$ ergs, sufficient to produce an input of $\sim 10^{39}$ ergs s^{-1} if the particles can escape. However, the mean spectral index of the remnants, -0.45, would produce a cosmic ray electron spectrum of 1.9, significantly different from the observed value of 2.5. Therefore, although sufficient energy for the electron component of cosmic rays is in principle available from supernovae, a mechanism must be found to explain the difference in spectra. To supply the cosmic ray photons would require an injection rate of 1×10^{50} ergs per event. Such energy is available at the time of the outburst, at least in the Colgate-White model where the outer envelope is ejected at relativistic speeds. However, recent observations of the chemical composition and anisotropy of cosmic rays lead to the suggestion that the protons at least may be of extragalactic origin (Brecher and Burbidge 1972).

5.6   SUMMARY

Much progress has been made in the identification of supernova
remnants, and in the study of their radio properties. The number of such
objects known will probably not increase significantly in the next several
years, although it would be important to find a few large remnants that
are in the third and final stage of evolution. Perhaps one such object
is the Gum Nebula. Future observations should concentrate on

1) the measurement of the polarization structure at radio wavelengths,
   in order to determine more clearly the interaction between the
   remnant and the interstellar gas;

2) optical studies of filaments in remnants, in order to obtain
   distances and, perhaps, to distinguish the type of supernova
   and the stage of evolution of the remnant;

3) X-ray studies of the remnants, in order to determine if particle
   injection is still continuing, and to distinguish the stage of
   evolution of the remnant by measuring the temperature of the
   material inside the shell.

From the standpoint of theory, the stages of hydrodynamic evolution
are generally understood, but a much more detailed model of the second stage,
where the shell is decelerated by the ambient interstellar matter would be
most useful. In addition, the work by Pacini on the relationship between
pulsars and remnants, especially relating to continuing injection of
particles, should be followed up.

REFERENCES

Baade, W. and Minkowski, R. 1954, Astrophys. J. 119, 206.

Baldwin, J. E. 1971, IAU Symp. 46: The Crab Nebula, D. Reidel Publishing Co.,
Dordrecht, p. 22.

Bergh, S. van den 1971, Astrophys. J., 168, 37.

Bergh, S. van den, and Dodd, W. W. 1970, Astrophys. J. 162, 485.

Bolton, J. G., Stanley, G. J., and Slee, O. B. 1949, Nature, 164, 101.

Brecher, K., and Burbidge, G. R. 1972, Astrophys. J. 174, 253.

Cocke, W. J., Disney, M. J. and Taylor, D. J. 1969, Nature 221, 525.

Colgate, S. A., and White, R. H. 1966, Astrophys. J. 143, 62.

Colgate, S. A. 1972, Astrophys. J. 174, 377.

Davidson, K. and Tucker, W. 1970, Astrophys. J. 161, 437.

Dickel, J. R.,and Milne, D. K. 1972, Australian J. Phys. (in press) 25,537

Dombrovsky, V. A. 1954, Dokl. Akad. Nauk., 94, 1021.

Downes, D. 1971, Astron. J. 76, 305.

Downs, G. S., and Thompson, A. R. 1972, Astron. J. 77, 120.

Drake, F. D. 1970, Publ. Astron. Soc. Pacific 82, 395.

Duyvendak, J. J., Mayall, N. U., and Oort, J. H. 1942, Publ. Astron. Soc. Pacific,
54, 91.

Gold, T. 1969, Nature, 221, 25.

Goldreich, P. and Julian, W. H. 1969, Astrophys. J. 157, 869.

Gordon (Pecker-Wimel), Ch. 1972, Astron. Astrophys. 20, 87.

Gorenstein, P., Harris, B., Gursky, H., Giacconi, R., Novick, R. and
Van den Bout, P. 1971, Science 172, 369.

Hermann, B. R. 1971, Ph.D. Thesis, University of Illinois.

Hogg, D. E., Macdonald, G. H., Conway, R. G., and Wade, C. M. 1969,
Astron. J. 74, 1206.

Ilovaisky, S. A. and Lequeux, J. 1972a, Astron. Astrophys. 18, 169.

_____ 1972b, Astron. Astrophys. 20, 347.

Jennison, R. C. 1965, Nature, 207, 740.

Jura, M. and Dalgarno, A. 1972a, Astrophys. J. 174, 365.

_____ 1972b, ibid, 1.

Kesteven, M. J. L. 1968, Australian J. Phys. 21, 739.

Kowal, C. T. 1968, Astron. J. 73, 1021.

Kundu, M. R. 1969, Astrophys. J. 158, L103.

Lang, K. R. 1971, IAU Symp. 46: The Crab Nebula, D. Reidel Publishing Co.,
    Dordrecht, p. 91.

Mayer, C. H. and Hollinger, J. P. 1968, Astrophys. J. 151, 53.

Miller, J. S. and Wampler, E. J. 1969, Nature, 221, 1037.

Milne, D. K. 1970, Australian J. Phys. 23, 425.

Minkowski, R. 1968, Nebulae and Interstellar Matter, ed. B. M. Middlehurst
    and L. H. Aller, University of Chicago Press, Chicago, p. 623.

Minkowski, R. 1971, IAU Symp. No. 46: The Crab Nebula, D. Reidel Publishing
    Co., p. 241.

Morrison, P. and Sartori, L. 1969, Astrophys. J. 158, 541.

Novick, R., Weisskopf, M. C., Berthelsdorf, R., Linke, R., and Wolff, R. S.
    1972, Astrophys. J., 174, L1.

Ostriker, J. P., and Gunn, J. E. 1969, Astrophys. J. 157, 1395.

Pacini, F. 1971, IAU Symp. 46: The Crab Nebula, D. Reidel Publishing Co.,
    Dordrecht, p. 394.

Parker, R. A. R. 1964, Astrophys. J. 139, 493.

Peimbert, M. and van den Bergh, S. 1971, Astrophys. J. 167, 223.

Poveda, A. and Woltjer, L. 1968, Astron. J. 73, 65.

Rosenberg, I. 1970, Mon. Not. Roy. Astron. Soc. 151, 109.

Scargle, J. D. 1969, Astrophys. J. 156, 401.

Scott, P. F., Shakeshaft, J. R. and Smith, M. A. 1969, Nature, 223, 1139.

Shklovsky, I. S. 1954, Dokl. Akad. Nauk. 98, 353.

Shklovsky, I. S. 1960, Soviet Astron. 4, 243.

Shklovsky, I. S. 1968, Supernovae, John Wiley and Sons, New York.

Staelin, D. H. and Reifenstein, E. C. 1968, Science 162, 1481.

Tammann, G. A. 1970, Astron. Astrophys. 8, 458.

Trimble, V. 1968, Astron. J. 73, 535.

van der Laan, H. 1962, Mon. Not. Roy. Astron. Soc. 124, 125.

Vashakridze, M. A. 1954, Astron. Tsink 147, 11.

Weiler, K. W. and Seielstad, G. A. 1971, Astrophys. J. 163, 455.

Woltjer, L. 1958, Bull. Astron. Inst. Neth. 14, 39.

Woltjer, L. 1970a, Publ. Astron. Soc. Pacific 82, 479.

Woltjer, L. 1970b, IAU Symp. 39: Interstellar Gas Dynamics

    D. Reidel Publishing Co., Dordrecht, p. 229.
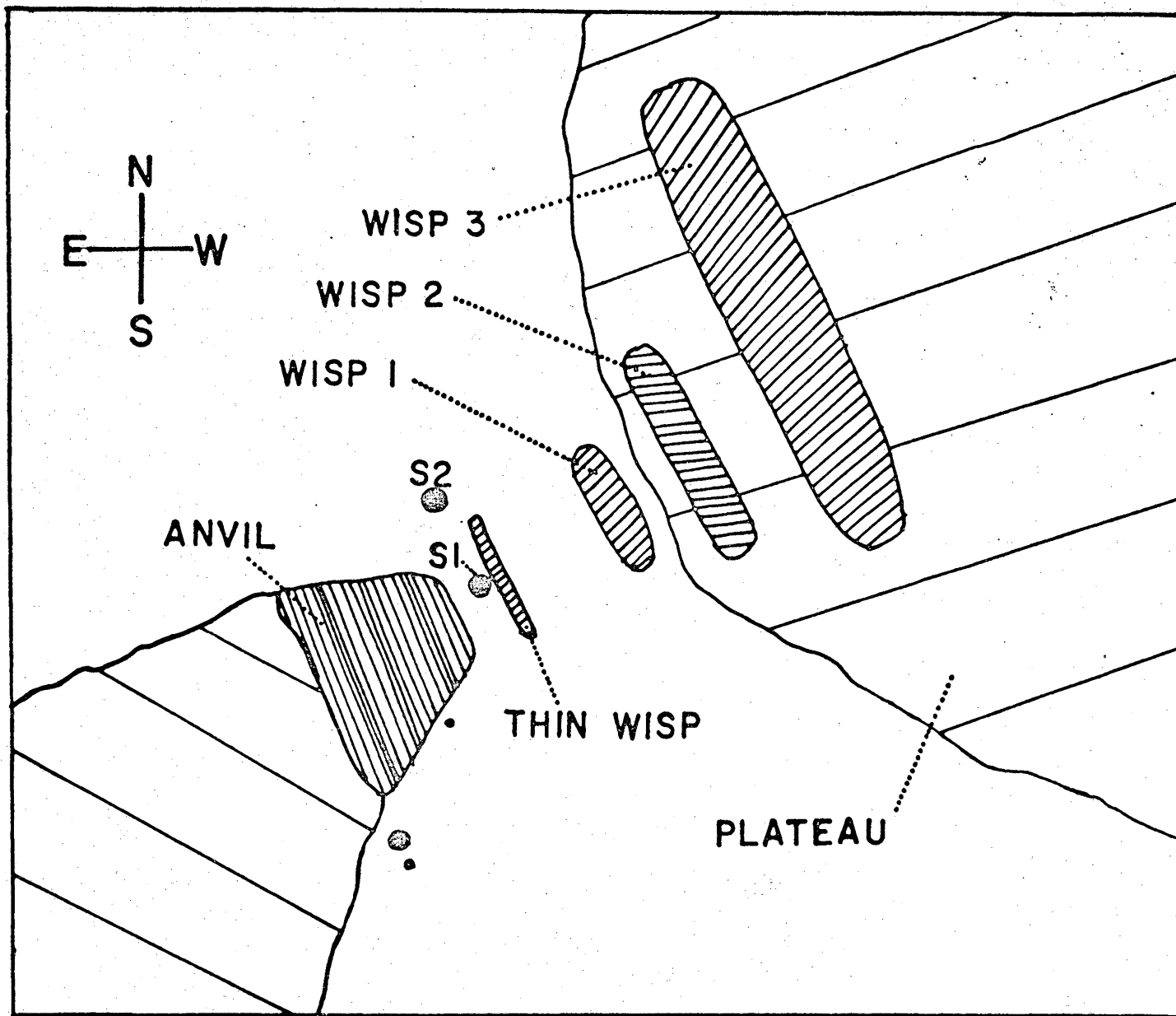
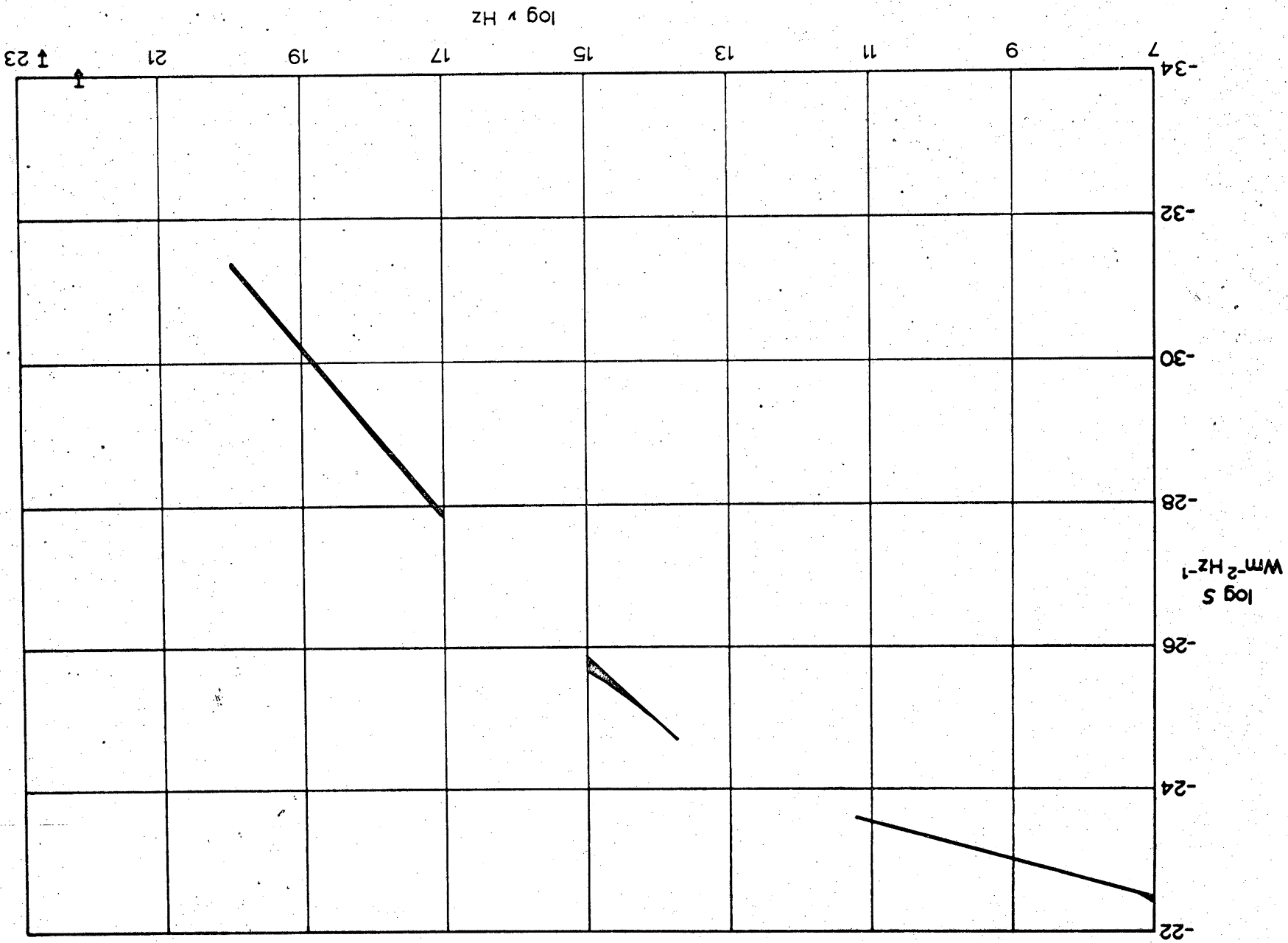Woltjer, L. 1972, Ann. Rev. Astron. Astrophys. 10, 129.

CAPTIONS TO FIGURES

Fig. 5.1   Schematic representation of the nebulosity and stars in the
            central region of the Crab Nebula.

Fig. 5.2   The brightness distribution over the Crab Nebula at a wavelength
            of 11.1 cm. The coordinates are for 1950.0. The contour
            interval is 620 °K, and the outermost contour level is 2200 °K.

Fig. 5.3   The electromagnetic spectrum of the total radiation from the
            Crab Nebula. The thickness of the lines indicates the uncertainty
            at a given frequency.

Fig. 5.4   The central region of the Crab Nebula, with north at the top
            and east to the left. The upper picture is taken when the
            pulsar is near minimum light, and shows the north-preceding
            star S2. The lower picture shows the pulsar near maximum light.

Fig. 5.5   The brightness distribution over Cas A at a wavelength of 11.1 cm.
            The coordinates are for 1950.0. The contour interval is 1750 °K,
            and the outermost contour level is 5200 °K.

Fig. 5.6   Intrinsic position angle of the electric vector for Tycho's
            supernova. The solid line shows the distribution of intensity
            of the 21.1 cm polarized radiation, at a level of 0.012×10^{-26} W m^{-2}
            Hz^{-1} per square min of arc, while the dashed line shows the 10.4 cm
            contour, at a level of 0.029×10^{-26} W m^{-2} Hz^{-1} per square min of
            arc.

Fig. 5.7   Distribution of antenna temperature at 40 cm over the Cygnus Loop.
            The contour unit is 0.75 °K.

Fig. 5.8   The surface brightness Σ as a function of linear diameter D for the
            sixteen remnants from Table 1. The least-squares solution $\Sigma \propto D^{-3.7}$
            is also shown.

TABLE 5.1
Radio Properties of Remnants of Known Distance

Galactic Source Number	Source	Flux at 1 GHz flux units	Spectral Index	Mean Diameter Arc min	Surface Brightness 1 GHz (MKS)	Distance kpc	Diameter pc
G111.7-2.1	Cas A	3100	-0.77	4.3	2.00E-17	3.0	3.8
G184.6-5.8	Tau A	1000	-0.25	3.6	9.18E-18	2.0	2.1
G 4.5-6.8	Kepler	20	-0.58	3.0	2.64E-19	6 - 10	5 - 9
G 43.3-0.2	W49B	39	-0.33	4.8	2.02E-19	10	14
G326.2-1.7	MHR44	145	-0.24	9.8	1.80E-19	4	11
G130.7+3.1	3C58	33	-0.10	6.3	9.89E-20	8	15
G120.1+1.4	Tycho	52	-0.74	8.1	9.43E-20	5	12
G 41.1-0.3	3C397	35	-0.3	9.0	5.14E-20	7	18
G332.4-0.4	RCW103	28	-0.34	9.0	4.11E-20	4	10
G 34.6-0.5	W44	190	-0.40	31	2.29E-20	3	27
G189.1+2.9	IC443	180	-0.45	40	1.34E-20	1 - 2	12 - 23
G263.4-3.0	Vela XYZ	1800	-0.30	200	5.35E-21	0.5	29
G327.6+14.5	SN1006	25	-0.63	26	4.40E-21	1.3	10
G315.4-2.3	RCW86	33	-0.5	40	2.45E-21	2.5	29
G132.4+2.2	HB3	36	-0.7	80	6.70E-22	2.0	46
G74.0-8.6	Cygnus Loop	160	-0.45	180	5.94E-22	0.8	42

N

E — W

S

WISP 3

WISP 2

WISP 1

S2

ANVIL

S1

THIN WISP

PLATEAU

log ν Hz

23 21 19 17 15 13 11 9 7

-34 -32 -30 -28 -26 -24 -22

log S
Wm^{-2}Hz^{-1}